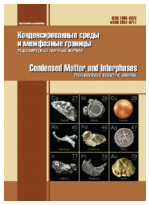

ISSN 1606-867X (Print)
ISSN 2687-0711 (Online)
Condensed Matter and Interphases
Kondensirovannye Sredy i Mezhfaznye Granitsy
https://journals.vsu.ru/kcmf/

Original articles

Research article
https://doi.org/10.17308/kcmf.2023.25/10970

Atomic composition, microstructure, and electromagnetic properties of schungite micropowder

V. Yu. Buz'ko, S. N. Ivanin ✉, I. Yu. Shutkin, A. I. Goryachko, S. A. Udodov, A. V. Ozolin

Kuban State Technological University,
2 Moskovskaya str., Krasnodar 350072, Russian Federation

Abstract

The goal of the work was to study the microstructural, elemental, and electromagnetic properties of the samples of micropowder made from a natural mineral schungite. It was found that according to an X-ray spectral microanalysis, the carbon content in the studied samples of the mineral schungite was from 44 to 54 wt% while the iron content did not exceed 3.9 wt%. The iron content increased up to 6.1 wt% in the produced schungite micropowder.

It can be presumed that in the schungite, micropowder iron exists in the form of ferrimagnetic nanoparticles of magnetite and pyrite, which is formed when grinding schungite particles in ball mills with a steel body and a milling bowl. The produced schungite micropowder also showed the presence of weak ferrimagnetic properties according to the measurements of magnetic permeability performed by vector analysis of the impedance of electrical circuits.

In accordance with its electromagnetic characteristics, schungite micropowder made from shungite mineral is an effective radio-absorbing filler for building materials for cellular communication frequency bands.

Keywords: Schungite, Elemental composition, Microstructure, Electromagnetic characteristics, Building materials

Funding: The research was partially supported by the Kuban Science Foundation and the Kuban State Technological University as part of the scientific project No. MFI-P-20.1/9 "Development and research of building and construction materials with special electromagnetic properties".

For citation: Buz'ko V. Yu., Ivanin S. N., Shutkin I, Yu., Goryachko A. I., Udodov S. A., Ozolin A. V. Atomic composition, microstructure, and electromagnetic properties of schungite micropowder. *Condensed Matter and Interphases*. 2023;25(1): 3–13. https://doi.org/10.17308/kcmf.2023.25/10970

Для цитирования: Бузько В. Ю., Иванин С. Н., Шуткин И. Ю., Горячко А. И., Удодов С. А., Озолин А. В. Атомный состав, микроструктура и электромагнитные свойства микропорошка шунгита. *Конденсированные среды и межфазные границы*. 2023;25(1): 3–13. https://doi.org/10.17308/kcmf.2023.25/10970

✉ Sergey N. Ivanin, e-mail: Ivanin18071993@mail.ru

1. Introduction

Schungite is a unique natural carbon-containing mineral with a hybrid microstructure the proven reserves of 38-40 million tons of which are located in Karelia [1–3]. The total reserves of schungite rocks in Karelia is estimated to be several billion tons [4, 5]. It is known that the mineral content of schungite-containing rocks is formed by nanostructured schungite carbon, quartz, silicates (sericite, chlorite, feldspars), carbonates (siderite and dolomite), and sulphides (pyrite, pyritine, sphalerite, and chalcopyrite) [1-7]. The main chemical components of schungite rocks are schungite carbon with the content from 15 to 50 % [1, 3, 7], silica in the form of quarts of various modifications with the content from 25 to 75 % [1, 2], and pyrite with the content from 2 to 5.8 % [8–11].

Schungite rocks are natural microheterogeneous composite materials with various nanostructured forms of carbon. Being nano-sized structures of different nature, schungite is considered to closely cover the surface of mineral particles of jointly present minerals with a film in the form of flakes [4–7, 12]. Due to the high content of the electrically conductive carbon phase [4–7, 12], schungite materials in the form of small particles or micropowders can be used as a dielectric filer for the production of radio-absorbing and radio-shielding composite materials [4–7, 12]. For example, schungite in the form of ground particles and micropowders is used as a dielectric filer in radio-absorbing construction materials [13–20] and radio-shielding concrete compositions [21–23].

Scanning electron microscopy (SEM) is widely used in practical material science to study a wide range of heterogeneous materials, such as metal, composite, building, and geological materials. This is due to the fact that the obtained images of the microstructure are of high quality and the process of preparation of the objects for microscopic studies is relatively simple and does not require long sample preparation. In case of natural minerals and rocks, the combination of the SEM method and microprobe analysis provides great potential for studying the structural features of the microstructure and phase microheterogeneity of minerals and mineral raw materials [25].

As for electron microscopy of rocks and raw building materials, the signal of the so-called "secondary electrons", the electrons of atoms emitted from the sample as a result of inelastic scattering (*secondary electron image* – SEI) [25, 26], is most often used to obtain images of particles. Secondary electrons are electrons with low energy, which is less than 50 eV, as they are mostly formed only in the ultrathin surface layer of the material up to 10 nm [28]. Is is known that secondary electrons allow obtaining a higher resolution (< 10 nm) signal, than in the case of the analysis of backscattered electrons signals [26].

A special mode (*backscattered electron image* – BEI) of signal registration by backscattered electrons is used to obtain the information on the surface distribution of phases in the studied samples when using SEM [25, 26]. In this mode, which can be named BSE, COMPO, or BSD depending on the manufacturer of the electronic microscope, image contrast is formed by backscattered electrons based on the difference between average atomic masses of the sample's components in the studied regions or phases [25, 26]. The emission of backscattered electrons significantly depends on the atomic number and, correspondingly, the atomic mass of the chemical elements. The greater the value of the average atomic mass of the studied area of the sample is, the greater the number of electrons are backscattered from these atoms at a smaller depth in the sample when the sample is exposed to the probing beam. Correspondingly, the areas of the sample with smaller average atomic masses look darker on the photo of the microstructure. Recently, the electron microscopy in backscattered electrons has been widely used in material science for construction and raw materials [27, 28].

In a number of works [5, 6, 12, 16], schungite powders used as a radio-absorbing filler for building and construction materials were considered as purely dielectric radio-absorbing fillers with electrically conductive carbon particles. However, doubts occur as to whether this assumption is correct as iron is known to be present in schungite rocks in the form of particles of such minerals as pyrite, magnetite, and siderite and iron hydroxides [2, 3, 5, 9–11]. At least one of these forms of iron, natural magnetite, is a pronounced ferrimagnetic material [29, 30] while natural pyrite has a mixture

of both weak ferrimagnetic and paramagnetic properties [31, 32].

The goal of the work was to study the microstructural, elemental, and electromagnetic properties of the samples of the micropowder made of a natural mineral schungite. Such a powder can be used as a highly-permeable dielectric filler to create eco-friendly building radio-absorbing materials, therefore, a comprehensive study of its properties is relevant.

2. Experimental

2.1. The studied schungite samples

Samples of schungite mineral (produced in the Russian Federation) in the form of particles 2 to 12 mm in size from the schungite rock of the Zazhoginsky deposit were purchased commercially at different times in different batches (Table 1).

We produced a sample of schungite powder made from the particles of the mineral from sample No. 2 as it showed a smaller content of carbon, which is important for durability of concrete compositions based on it. The schungite micropowder was obtained through mechanic abrasion of schungite particles in in a ball mill MSHL-1 with a drum and milling balls made of non-magnetic stainless steel AISI SS304 in the course of 4 hours and through sifting of the obtained powder with a sieve with cell sizes of 100μm. Such a method of preparation of schungite micropowder allowed simulating the contamination of the powder with iron compounds which inevitably appear due to abrasion of schungite particles in a ball mill with the most common steel drum and steel/cast-iron milling bowl.

2.2. Scanning electron microscopy and elemental analysis

The microstructure of schungite samples was studied using a scanning electron microscope EVO HD15 (ZEISS) with both modes of secondary electrons (SEI) and backscattered electrons (BSD). The BSD mode was chosen due to the fact that in this case the image reflects real phase composition of the sample and has a good phase contrast. The qualitative elemental analysis and mapping of the distribution of chemical elements were conducted using an INCA X-Max energy dispersive microanalysis attachment (Oxford Instruments) to the scanning electron microscope. The samples for measurements were placed on carbon tape with special duralumin holders. The elemental composition of each sample was measured three times in different areas, and the results were statistically averaged.

Table 1. The studied schungite samples

Sample	Description	Particle size	Manufacturer
№ 1	mineral particles	5–12 mm	OOO "SHUGGE"
№ 2	mineral particles	2–5 mm	OOO NPK Karbon-Shungite
№ 3	micro-powder	<100 mkm	Self-made

2.3. VNA measurements.

To determine the electromagnetic properties of the produced schungite micropowder, we measured the characteristics of losses upon reflection based on its composite with paraffin with mass fraction of the filler of 50 % in a 10-cm HP-11566A coaxial cell with the size of a toroid of 7.0×3.05 mm using a KC901V Deepace dual-port vector network analyser in the frequency range of 15 MHz to 7.0 GHz.

According to the theory of power lines, the damping constant of an electromagnetic wave in a material can be determined as follows [33]:

$$\gamma = j\frac{2\pi f}{c}\sqrt{\varepsilon\mu}, \quad (1)$$

where f is the frequency of the electromagnetic wave, c is the speed of light, ε and μ are the complex dielectric and magnetic permeability of the material.

Thus, the more the value (ε·μ) is, the more effective the electromagnetic wave is absorbed in this material with frequency f.

In the case of a perfect quarter wave electromagnetic absorber, the relationship between the frequency of maximum radio absorption f_m and its electromagnetic characteristics is determined by the following formula [34]:

$$f_m = \frac{c}{4d_m}\frac{1}{\sqrt{\varepsilon'\mu'}}\left(1+\frac{1}{8}\tan^2 r_\mu\right), \quad (2)$$

where d_m is the thickness of the absorbing layer, c is the speed of light, ε′ and μ′ are the real parts

of the dielectric and magnetic permeability of the material, tan r_μ is the magnetic loss angular tangent.

Taking into account the fact that schungite is not a pronounced magnetic material and that for its composite with paraffin a simplified formula can be obtained to describe the relationship between the peak frequency of maximum radio absorption f_m of the material and its electromagnetic characteristics [34]:

$$\sqrt{\varepsilon\mu} = \left(4 f_m d_m / nc\right), \qquad (3)$$

where n = (1, 3, 5...) for the cases of resonant reflection of electromagnetic waves.

Magnetic permeability of the sample of a composite produced from the obtained schungite powder with paraffin was calculated by the experimental measurement of S-parameter S_{21} using a dual-port vector network analyser through the calculation of the corresponding impedance of electrical circuit Z [35–37], taking into account that with the used equipment Z_0 = 50 Ohm:

$$\mathrm{Z} = \mathrm{Z}_0 \frac{2\left(1 - S_{21}\right)}{S_{21}}. \qquad (4)$$

The approach of calculating the impedance of an electric circuit from the transmission parameter S_{21}, as compared to its calculation from the parameter S_{11}, is believed to provide more accurate values of the magnetic permeability of samples from the impedance of the circuit in a wide frequency range from 1 MHz to 6.5 GHz [36, 37].

Using the obtained frequency dependence of the impedance of circuit Z, we calculated the magnetic permeability of sample μ according to the following formula [36, 37]:

$$\mu = \mu' - j\mu'' = 1 + \frac{Z - Z_{\mathrm{air}}}{jhf\mu_0 \ln\left(r_2 / r_1\right)}, \qquad (5)$$

where Z and Z_{air} are the values of the complex impedance of the circuit with the coaxial cell used in the presence and absence of the studied toroidal sample, h is the height of the toroidal sample, f is the frequency of electromagnetic radiation, μo is the magnetic permeability of free space, and r_2 and r_1 are the outer and inner radii of the toroidal sample.

3. Results and discussion

The microstructure of the surface of the studied schungite mineral is presented in Fig. 1. It was found that the studied samples of schungite mineral contained a nanostructured phase with an average size of nanoparticles of 85 ± 30 nm. According to the data of electron microscopy, such nanoparticles are grouped in submicrosized aggregates which fill the pores, fractures, and edge regions of microparticles of forming minerals. Thus, the images of the schungite surface obtained in secondary electrons provide information on the presence of pronounced microheterogeneities, large pores, and surface relief in the studied material.

To study the microheterogenous state of the schungite sample No. 1, we selected the BSD mode of backscattered electrons as in this case the image reflects the real phase composition of a sample and, as compared to the SEI mode of secondary

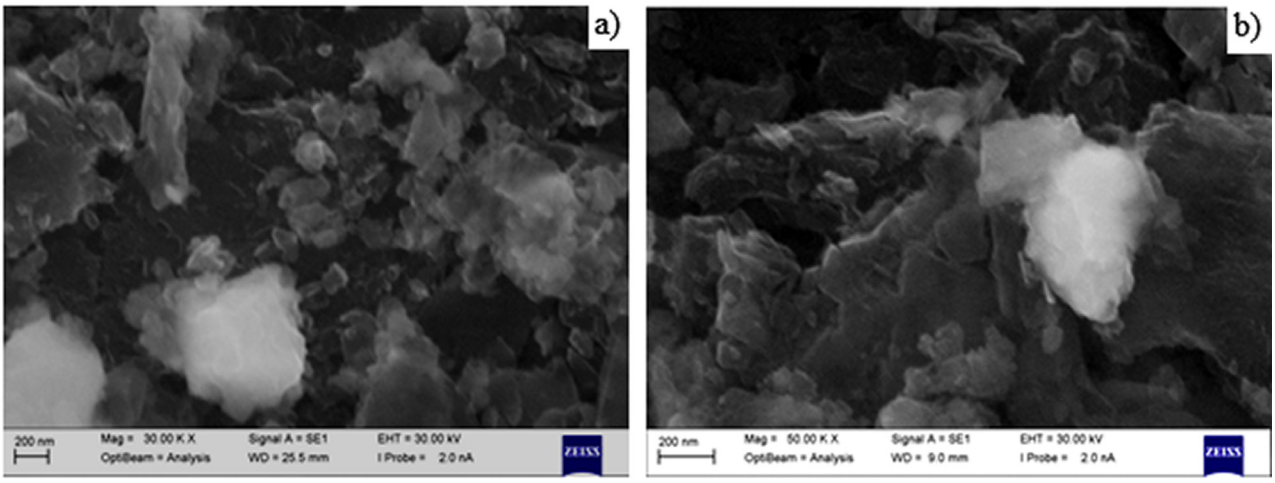

Fig. 1. Photos of the microstructure of the surface of the schungite mineral: a – sample No. 1; b – sample No. 2

electrons, it allows obtaining an image with a high phase contrast. The back reflected electrons were recorded by two semiconductor detectors located directly above the sample. In the BSD mode, the signals of two detectors were summed, which allowed minimising the influence of the relief irregularities on a raster image. Therefore, the total signal was mostly dependent on the change of the average atomic number, that is on the composition of the studied area of the sample.

Photos of the microstructure of the surface of the schungite mineral in the mode of backscattered electrons are presented in Fig. 2. According to the data in Fig. 2, in these photographs the phases based on elements with a small atomic mass (C, O, Al, Si) are dark areas while phases based on elements with a large atomic mass (Fe, S) correspond to light areas.

It can be seen that the ferric sulphide (in the form of a FeS_2 pyrite) in sample No. 1 was represented by the particles with the size of 200–300 nm while in sample No. 2 the ferric sulphide was represented by the particles of smaller sizes between 100 and 220 nm. Therefore, microscopic images of the schungite surface obtained in backscattered electrons provided information on the presence of a pronounced heterogeneous microstructure in the material.

Energy-dispersive X-ray spectroscopy microanalysis (EDS) allowed identifying relative concentrations of chemical elements in the schungite samples and reflect the distribution of chemical elements on the surface of the studied samples (Fig. 3).

According to the data of Fig. 3, there was a pronounced microheterogeneity of phases on the surface of the studied schungite mineral, and the association of iron and sulphur with the formation of pyrite microcrystals could also be observed. However, some atoms of sulphur did not have any direct relation with the location of iron atoms and it was most likely associated with the microphase of gypsum particles $CaSO_4 \cdot 2H_2O$.

The elemental composition of the studied schungite samples and its powder prepared according to the EDS data is presented in Table 2.

The obtained results on the elemental composition of schungite correlate well with the experimental data of other previous works [1, 2, 5–11]. It was discovered that the iron content in the studied schungite samples was relatively low and did not exceed 3.8 wt%. It is considered [1–3, 5–11] that iron is present in schungite rocks in the form of pyrite, magnetite, siderite, and iron hydroxides. Based on the obtained elemental ratios and the data from previous works [1–3, 5–11], we can conclude that in the studied samples of the schungite mineral, iron is partially found in the form of iron disulphide FeS_2 (pyrite), both as the main iron-containing mineral in schungites in accordance with [9-11] and in the form of iron oxides Fe_2O_3 (hematite) and Fe_3O_4 (magnetite).

According to the data of Table 2, milling schungite mineral sample No. 2 into sample No. 3 in a ball mill resulted in an increase of the share of elemental iron in it by 60 %. The

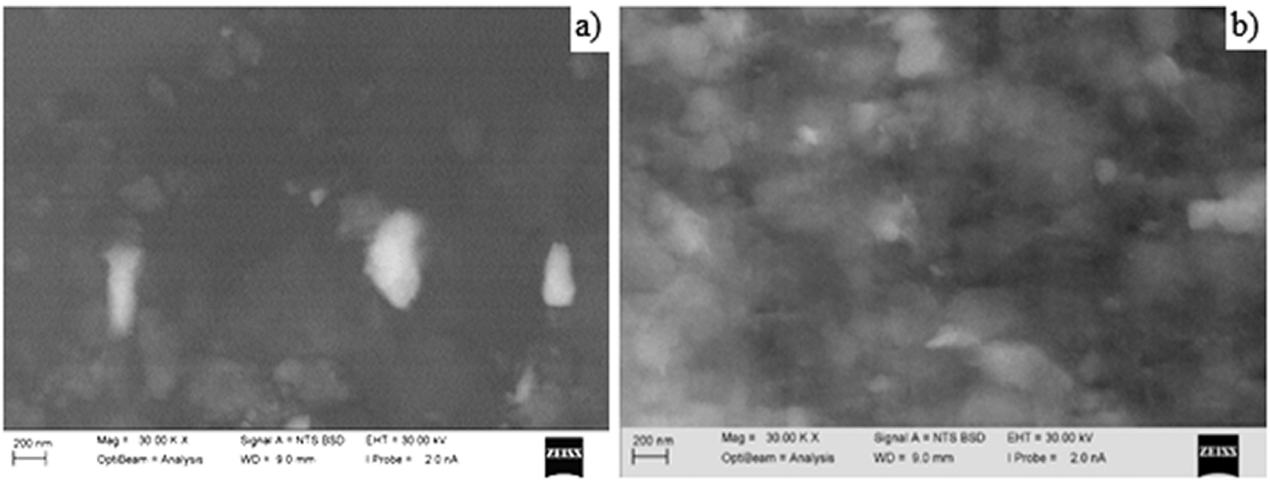

Fig. 2. Photos of the microstructure of the surface of the schungite mineral in the mode of backscattered electrons: a – sample No. 1; b – sample No. 2

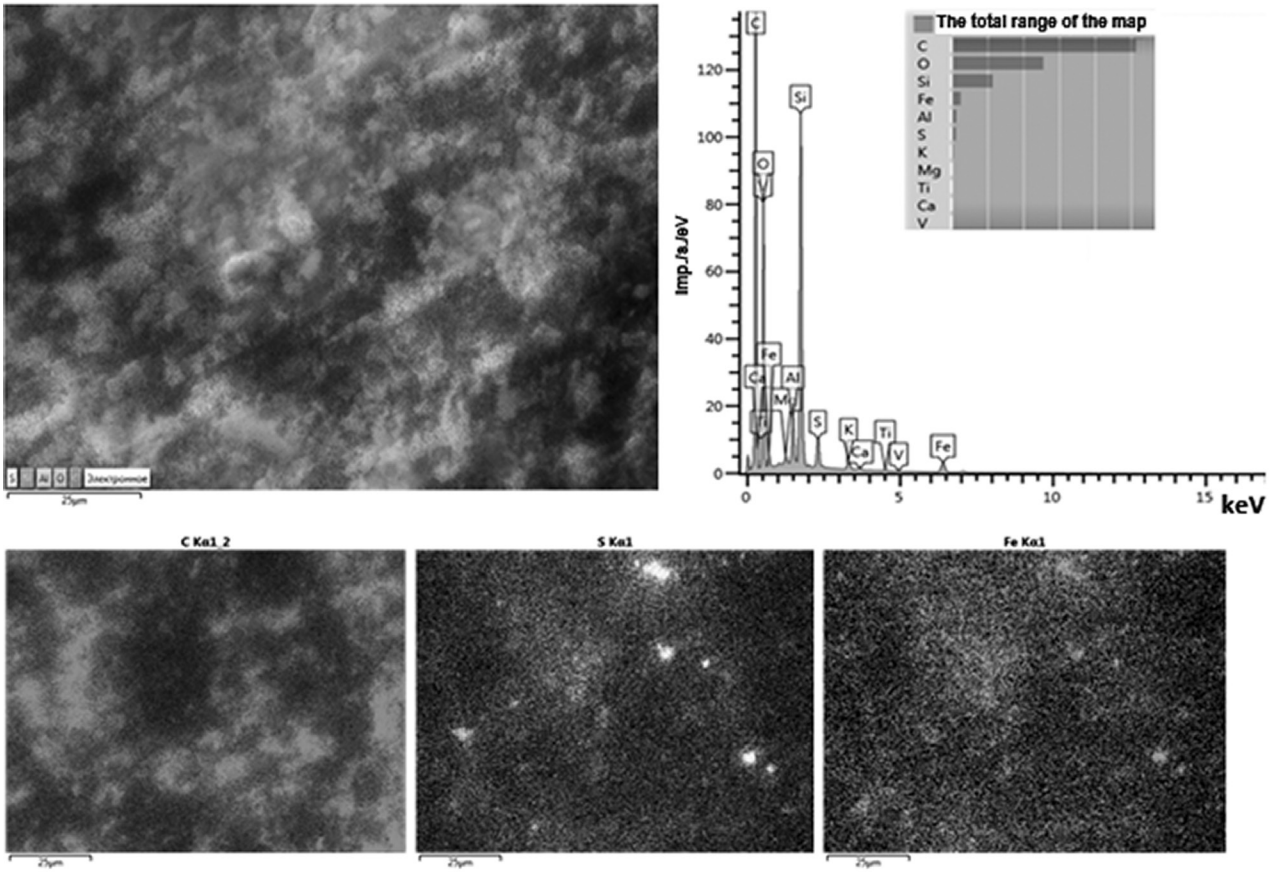

Fig. 3. The distribution of chemical elements on the surface of the schungite mineral No. 1 and the corresponding EDS spectrum

Table 2. Elemental composition of the studied schungite samples

Element	№1 (wt%)	№1 (at%)	№2 (wt%)	№2 (at%)	№3 (wt%)	№3 (at%)
C	50.91±0.19	63.77±0.24	44.11±1.22	57.01±1.58	32.34±3.78	43.80±5.12
O	27.72±0.12	26.07±0.11	31.79±0.88	30.85±0.85	43.24±2.91	43.97±2.96
Mg	0.36±0.03	0.22±0.02	0.20±0.09	0.13±0.06	0.14±0.10	0.09±0.06
Al	2.36±0.06	1.32±0.03	1.74±0.12	1.00±0.07	1.46±0.41	0.88±0.25
Si	11.59±0.12	6.21±0.06	16.57±0.45	9.16±0.25	14.89±1.09	8.62±0.63
S	1.77±0.07	0.83±0.03	0.98±0.12	0.47±0.06	1.05±0.22	0.53±0.11
K	1.07±0.05	0.41±0.02	0.82±0.14	0.33±0.06	0.80±0.15	0.33±0.06
Ca	0.25±0.03	0.09±0.01	–	–	–	–
Ti	0.22±0.03	0.07±0.01	–	–	–	–
V	0.04±0.02	0.01±0.01	–	–	–	–
Fe	3.68±0.11	0.99±0.01	3.80±0.22	1.06±0.18	6.08±1.53	1.77±0.45
Ni	0.04±0.02	0.01±0.01	–	–	–	–

increased elemental content of iron in the produced schungite powder was associated with the technological features of obtaining schungite micropowders through grinding pieces of schungite-containing rock in a ball mill with a steel milling bowl. Apparently, due to the process of mechanical oxidation of iron sulphide to sulphate ions and elemental iron to carbonate ions, the shares of carbon, aluminium, magnesium, silicon, and potassium systematically lowered. A considerable decrease in the proportion of carbon in sample No. 3 can also be associated with the formation of ultra-high dispersive carbon upon grinding which is

intensively lost in the course of sifting of the ground schungite micropowder.

To study the microheterogenous state of the produced schungite powder (Fig. 4), we selected the BSD mode of backscattered electrons as in this case the image reflected the real phase composition of a sample and, as compared to the SEI mode of secondary electrons, it allowed receiving an image with a high phase contrast.

The observation of the produced schungite micropowder in the BSD mode showed its pronounced microheterogeneity. It can be seen that the carbon and oxygen phases are distributed unevenly, and these areas are the darkest. The formation of multiple faults and edge cleavages of microparticles is also typical. In the course of schungite grinding, multiple point areas with lowered content of carbon appear (Fig. 4, BSD – light areas). Therefore, according to the obtained experimental data of electron microscopy and EDS, significant microheterogeneity can be found in the distribution of chemical elements on the surface of the particles of the studied schungite powder sample. These results confirm that schungite mineral is a natural microheterogeneous composite material.

The frequency spectra of the radio absorption of the studied composite that are based on the produced schungite micropowder were processed and the results are presented in Fig. 5. It can be seen that there is a systemic shift of the resonance peak of radio absorption to the low frequency region upon an increase in the thickness of the sample.

It can also be observed that maximum losses upon reflection in the frequency range of 2 to 6.2

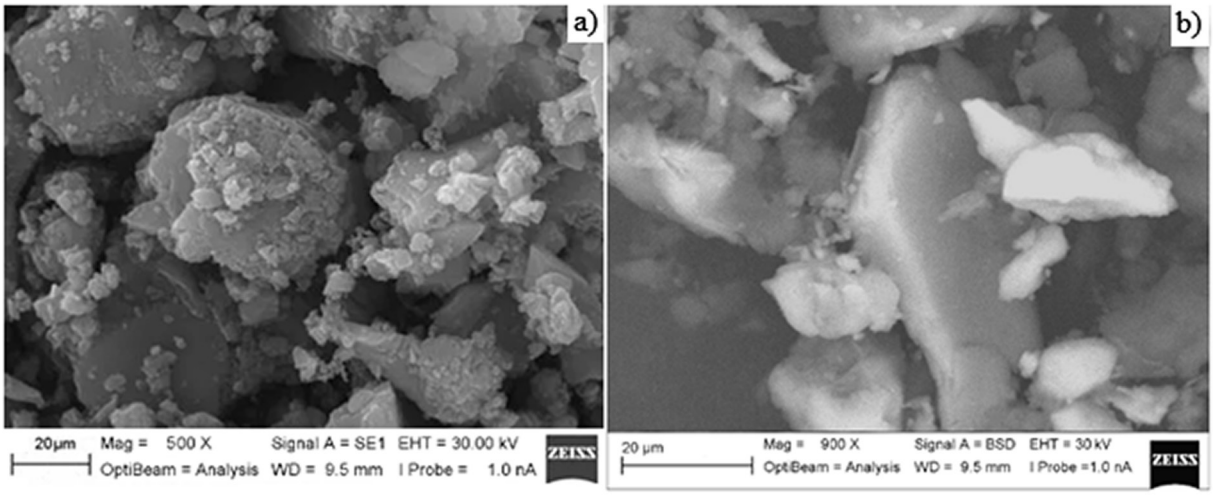

Fig. 4. Photos of the surface of particles of prepared schungite micropowder: a – in SEI mode; b – in BSD mode

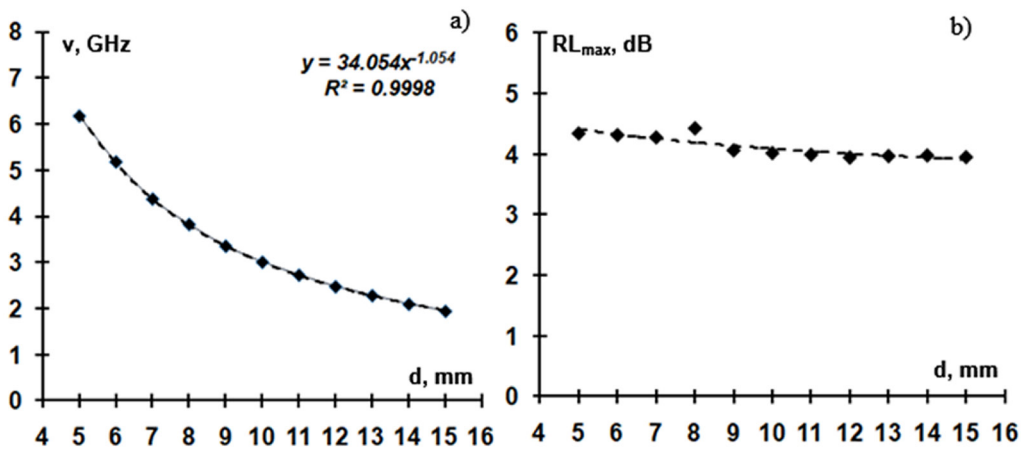

Fig. 5. Dependence of the resonance frequency (a) and the radio absorption peak (b) for the paraffin-schungite composite (50 wt%) on the sample thickness

GHz of the studied paraffin-schungite composite (50 wt%) are approximately 4–4.4 dB. These values correspond to the reflection coefficient of power *R* at the level of 0.4-0.36, which corresponds well with the results in [13-16].

The frequency dependence of the calculated value for the paraffin-schungite composite (50 wt%) according to equation (3) is presented in Fig. 6.

According to the obtained data in Fig. 6, schungite micropowder is a more appropriate dielectric filler for concrete building materials as compared to previously studied dielectric radio-absorbing fillers, such as rice husk ashes [38] or brass micropowder [39]. This is associated with the observed comparative property of the radio absorption ability of schungite (value ε·μ) as compared to rice husk ashes and brass micropowder and good compatibility of schungite powder as a mineral metal-silicate material with concrete as compared to brass micropowder that shows a corrosion interaction with cement mixtures.

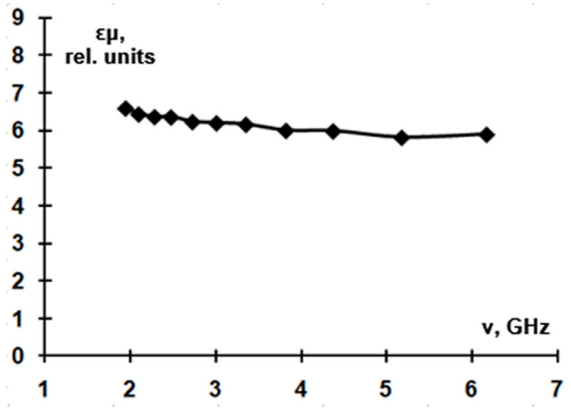

Fig. 6. Frequency dependence of the calculated value ε·μ for the paraffin-schungite composite (50 wt%)

This conclusion is confirmed by the comparison of the effectiveness of radio absorption by paraffin-based composites with the corresponding optimum quantity additives of the discussed radio-absorbing fillers for concretes (Fig. 7): powder of rice husk ashes (50 wt%), brass micropowder (10 wt%), and schungite micropowder (50 wt%).

According to the data in Fig. 7, a comparison of the radio absorption efficiency of paraffin-based composites with the corresponding additives of the discussed radio-absorbing fillers for concrete demonstrated a pronounced radio-absorption efficiency of the shungite-based composite for 4G and 5G cellular communication range.

Nevertheless, it should be taken into account that the produced schungite micropowder also showed the presence of weak ferrimagnetic properties μ ≫ 1 (Fig. 8) in accordance with the conducted calculations of the magnetic permeability based on the experimental measurement of the *S*-parameter S_{21} using the dual-port vector network analyser.

It can be presumed that it is associated with the presence of a small quantity of ferrimagnetic nanoparticles of magnetite Fe_3O_4 in the produced schungite micropowder which are probably formed upon the atmospheric dry milling of schungite particles in a steel ball mill with a steel milling bowl. This can be assumed based on the chemical features of the oxidation of stainless

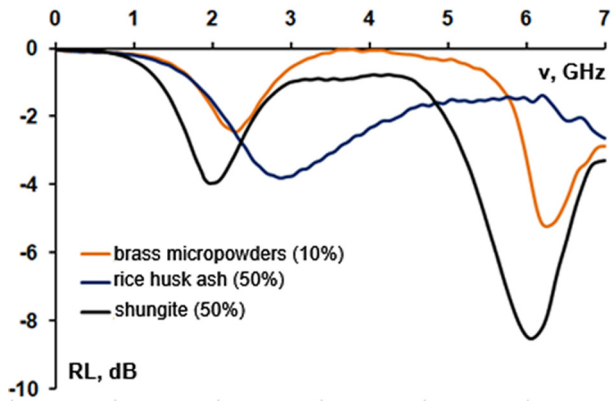

Fig. 7. Frequency dependence of reflection loss for composites based on paraffin and radio-absorbing fillers for concretes with a sample thickness of 15 mm

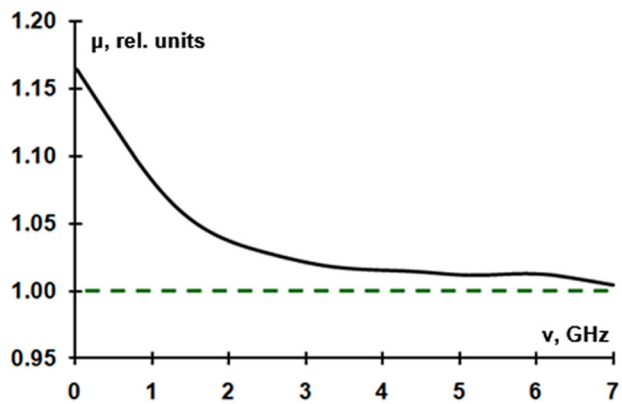

Fig. 8. Frequency dependence of the calculated value of magnetic permeability for the paraffin-schungite composite (50 wt%)

steel in the course of abrasion of abrasive metal powders in a ball mill with a drum and AISI SS304 non-magnetic stainless steel balls, as well as on the frequency behaviour of the high-frequency magnetic permeability calculated for the paraffin-schungite composite, which shows that Snoek's limit of the ferrimagnetic impurity is above 7 GHz. Therefore, the studied schungite micropowder cannot be considered as a purely dieletric radio-absorbing filler with electrically conductive carbon particles as is common in some works [5, 6, 12, 16, 40]. This conclusion corresponds well with the conclusion of [41], where it is stated that the frequency properties of the coefficients of reflection of electromagnetic radiation (EMR) from the surface of schungite-cement composites demonstrate a resonance effect at a frequency of 8.5 GHz, which can be explained by the content of metals in the structure of schungite and their impact on the reflection of EMR.

4. Conclusion

Thus, the conducted microscopic and energy spectral study of the schungite mineral and its produced micropowder showed that both the schungite itself and its micropowder contain significant concentrations of iron of 3.8 and 6.1 wt%, respectively. The schungite powder, apparently, contains iron in the form of ferrimagnetic nanoparticles of magnetite and pyrite, which also contributes to scattering and absorption of electromagnetic waves by schungite materials. The produced schungite micropowder also showed the presence of weak ferrimagnetic properties according to the measurements of magnetic permeability performed by vector analysis of the impedance of electrical circuits. This must be taken into account when discussing electromagnetic properties of industrially and independently produced schungite micropowders which are often used as radio-absorbing fillers for building materials.

Contribution of the authors

The authors contributed equally to this article.

Conflict of interests

The authors declare that they have no known competing financial interests or personal relationships that could have influenced the work reported in this paper.

References

1. Zavertkin A. S., Shchiptsov V. V. Technology for obtaining refractory and molding materials based on shungite rocks. *Scientific foundations of chemistry and technology for processing complex raw materials and synthesizing functional materials based on it**. 2008; 2. Available at: https://helion-ltd.ru/shungite-rocks-study/ (In Russ.)

2. Zavertkin A. S., Tyaganova V. I., Tupolev A. G. Application of chemicals and technological materials in pretreatment of shungite rock. In: *Problems in the rational use of natural and technogenic raw materials from the Barents region in the construction and technical material technology. Proceedings of Second International Conference 12–16 September,* 2005. p. 71–73. (In Russ., abstract in Eng.). Available at: http://resources.krc.karelia.ru/krc/doc/publ/problem_region_ispol/problem_region_ispol.pdf

3. Sadovnichy R. V., Rozhkova N. N., Gorbunova E. V., Chertov A. N. The Maksovskaya reserve (the Zazhoginskoye deposit) schungite rock photometric sorting possibilities study. *Obogashchenie Rud.* 2016;1: 10–15. (In Russ., abstract in Eng.). https://doi.org/10.17580/or.2016.01.02

4. Reznikov V. A., Polekhovskii Yu. S. Amorphous shungite carbon: A natural medium for the formation of fullerenes. *Technical Physics Letters*. 2000;26: 689–693. https://doi.org/10.1134/1.1307814

5. Golubev Y. A., Antonets I. V., Shcheglov V. I. Static and dynamic conductivity of nanostructured carbonaceous shungite geomaterials. *Materials Chemistry and Physics*. 2019;226: 195–203. https://doi.org/10.1016/j.matchemphys.2019.01.033

6. Antonets I. V., Golubev Y. A., Shcheglov V. I., Sun S. Electromagnetic shielding effectiveness of lightweight and flexible ultrathin shungite plates. *Current Applied Physics*. 2021;29: 97–106. https://doi.org/10.1016/j.cap.2021.06.008

7. Golubev E. V., Antonets I. V. Influence of mineralogical and petrographic features on microwave radiation reflection from shungite rocks in the range of 26–39 GHz. *Vestnik IG Komi SC UB RAS.* 2017;5: 43–48. (In Russ., abstract in Eng.). https://doi.org/10.19110/2221-1381-2017-5-43-48

8. Fujita T., Aoki T., Ponou,J., Dodbiba G., He C., Wang K., Ning S., Chen H., Wei Y. Removal of impurities from shungite via a combination of physical and chemical treatments. *Minerals*. 2021;11(3): 245. https://doi.org/10.3390/min11030245

9. Anufrieva S. I., Ozhogina E. G. Characteristics of the mineralogical and analytical study of natural types of shungite rocks. In*: The Significance of Technological Mineralogy Research in Solving the Problems of Integrated Development of Mineral Raw Materials*. Petrazavodsk: KarRC RAS. 2007. p. 135–145.

(In Russ.). Available at: http://resources.krc.karelia.ru/krc/doc/publ2008/mineralogia_135-145.pdf

10. Rafienko V. A. On the mechanism of leaching of sulfides from shungite rocks*. *Mining Informational and Analytical Bulletin (Scientific and Technical Journal)*. 2007;9: 38–48. (In Russ.). Available at: https://www.elibrary.ru/item.asp?id=9596187

11. Rafienko V. A., Yushin T. I. Development of technology for the processing of shungite rocks with the production of high quality dispersed shungite concentrates*. *Mining Informational and Analytical Bulletin (Scientific and Technical Journal)*. 2013;10: 102–110. (In Russ.). Available at: https://www.elibrary.ru/item.asp?id=20434286

12. Emelyanov S., Kuzmenko A., Rodionov V., Dobromyslov M. Mechanisms of microwave absorption in carbon compounds from shungite. *Journal of Nano- and Electronic Physics*. 2013;5(4): 40233. Режим доступа: https://www.elibrary.ru/item.asp?id=44952915

13. Lyn'kov L. M., Borbot'ko T. V., Krishtopova E. A. Radio-absorbing properties of nickel-containing schungite powder. *Technical Physics Letters*. 2009;35: 410–411. https://doi.org/10.1134/S1063785009050071

14. Pukhir G. A., Makhmud M. Sh., Nasonova N. V., Lynkov L. M. Protective properties of screens of electromagnetic radiation of a microwave range on the basis of the combined, dielectric and magnetic powder components. *Doklady BGUIR*. 2011;6(60): 94–97. (In Russ., abstract in Eng.). Available at: https://libeldoc.bsuir.by/bitstream/123456789/2005/1/Pukhir_Zashchitnyye.PDF

15. Lynkov L. M., Makhmud M. Sh., Krishtopova E. A. Screens of electromagnetic radiation based on powdered shungite. *Vestnik of Polotsk State University. Part C. Fundamental Sciences*. 2012;4: 103–108. (In Russ., abstract in Eng.). Available at: https://www.elibrary.ru/item.asp?id=23480159

16. Krishtopova E. A., Makhmud M. Sh., Lynkov L. M. Electromagnetic absorbers based on blends of powdered fillers. *Doklady BGUIR*. 2012;1(63): 17–21. (In Russ., abstract in Eng.). Available at: https://www.elibrary.ru/item.asp?id=29778573

17. Mukhametrahimov R. Kh., Shafigullin R. I., Kupriyanov V. N. Development of radioprotective shungite-containing gypsum-fiber facing sheets. *News of the KSUAE*. 2017;3(41): 224–231. (In Russ., abstract in Eng.). Available at: https://www.elibrary.ru/item.asp?id=30040186

18. Galautdinov A., Mukhametrakhimov R., Kupriyanov V. Gypsum-fiber radioprotective facing materials. *Lecture Notes in Civil Engineering*. 2021; 372–381. https://doi.org/10.1007/978-3-030-80103-8_40

19. Abdimuratov Zh. S., Manbetova Zh. D., Imankul M. N., Chezhimbayeva K. S., Davronbekov D. A. Absorbers of electromagnetic radiation based on shungite species. *Series of Geology and Technical Sciences*. 2021;445(1): 6–12. https://doi.org/10.32014/2021.2518-170x.1

20. Mosin O. V, Ignatov I. Application of natural fullerene containing mineral shungite in construction industry and building technologies. *Nanobuild*. 2012; 6: 81–93. (In Russ., abstract in Eng.). Available at: https://www.elibrary.ru/item.asp?id=18268370

21. Podolsky V. P., Volkov V. V., Kukina O. B., Andreev A. V. Substantiation of the possibility of using shungite as an effective radio-absorbing material. *Russian Journal of Building Construction and Architecture*. 2022;1(65): 69–75. (In Russ., abstract in Eng.). https://doi.org/10.36622/VSTU.2022.65.1.006

22. Lukutsova N. P., Pykin A. A., Karpikov E. G. Peculiarities of structure formation of cement stone with carbon-silica nanodispersed additive*. *Stroitel'nye Materialy (Construction Materials)*. 2011;9: 66–67. (In Russ.). Available at: https://www.elibrary.ru/item.asp?id=17247606

23. Belousova E. S., Makhmud M. M., Lynkov L. M., Nasonova N. V. Radio shielding properties of concretes based on shungite nanomaterials. *Nanobuild*. 2013;5(2): 56–67. (In Russ., abstract in Eng.). Available at: http://www.nanobuild.ru/en_EN/journal/Nanobuild-2-2013/56-67.pdf

24. Egerton R. F. *Physical principles of electron microscopy*. Springer Science+Business Media, Inc.; 2005. 211 p.

25. Reed S. J. B. *Electron microprobe analysis and scanning electron microscopy in geology*. New York: Published in the United States of America by Cambridge University Press; 2005 216 p.

26. Vlasov A. I., Elsukov K. A., Kosolapov I. A. *Electron microscopy: textbook*.* Moscow: Publishing House of MSTU im. N. E. Bauman; 2011. 168 p. (In Russ.)

27. Igarashi S., Kawamura M., Watanabe A. Analysis of cement pastes and mortars by a combination of backscatter-based SEM image analysis and calculations based on the Powers model. *Cement and Concrete Composites*. 2004;26(8): 977–985. https://doi.org/10.1016/j.cemconcomp.2004.02.031

28. Hu C., Ma H. Statistical analysis of backscattered electron image of hydrated cement paste. *Advances in Cement Research*. 2016;28(7): 469–474. https://doi.org/10.1680/jadcr.16.00002

29. Mashuri X., Lestari W., Triwikantoro X., Darminto X. Preparation and microwave absorbing properties in the X-band of natural ferrites from iron sands by high energy milling. *Materials Research Express*. 2018;5(1): 014003. https://doi.org/10.1088/2053-1591/aa68b4

30. Guan B., Ding D., Wang L., Wu J., Xiong R. The electromagnetic wave absorbing properties of cement-

based composites using natural magnetite powders as absorber. *Materials Research Express*. 2017;4(5): 056103. https://doi.org/10.1088/2053-1591/aa7025

31. Wu X., Xie X., Cao Y. Self-magnetization of pyrite and its application in flotation. *Transactions of Nonferrous Metals Society of China*. 2016;26(12): 3238–3244. https://doi.org/10.1016/s1003-6326(16)64456-4

32. Waters K. E., Rowson N. A., Greenwood R. W., Williams A. J. The effect of heat treatment on the magnetic properties of pyrite. *Minerals Engineering*. 2008;21(9): 679-682. https://doi.org/10.1016/j.mineng.2008.01.008

33. Yuping D., Hongtao G. *Microwave absorbing materials*. Singapore: Pan Stanford Publishing Pte. Ltd.; 2017. 387 p.

34. Liu L, Duan Y, Guo J. Influence of particle size on the electromagnetic and microwave absorption properties of FeSi/paraffin composites. *Physica B*. 2011;406(11): 2261–2265. https://doi.org/10.1016/j.physb.2011.03.045

35. Dosoudil R., Ušák E., Olah V. Computer controlled system for complex permeability measurement in the frequency range of 5 Hz – 1 GHz. *Journal of Electrical Engineering*. 2006;57(8/S): 105–109.

36. Dosoudil R., Ušák E., Olah V. Automated measurement of complex permeability and permittivity at high frequencies. *Journal of Electrical Engineering*. 2010;61(7/S): 111–114.

37. Dosoudil R. Determination of permeability from impedance measurement using vector network analyzer. *Journal of Electrical Engineering*. 2012;63(7s): 97–101.

38. Buz'ko V., Shamray I., Goryachko A., Udodov S., Abashin A. Electromagnetic characteristics of biosilica from rice husk. *E3S Web of Conferences*. 2021;263: 01013. https://doi.org/10.1051/e3sconf/202126301013

39. Buzko V. Yu., Udodov S. A., Litvinov A. E., Ivanin S. N., Goryachko A. I., Charikov G. Yu. Properties of radio-absorbing composites concrete-micropowders of the brass. *Scientific works of the Kuban State Technological University*. 2021;5: 25–33. (In Russ., abstract in Eng.). Available at: https://elibrary.ru/item.asp?id=47874005

40. Lisovskiy D. N., Mahmud M. S., Vlasova G. A., Pulko T. A. Absorbents of electromagnetic radiation based on the fire-proof paints with powder-like filler. *Doklady BGUIR*. 2012;4: 89–93. (In Russ., abstract in Eng.). Available at: https://elibrary.ru/item.asp?id=29425911

41. Belousova E. S., Lynkou L. M., Senyut V. T., Krishtopova E. A. Influence of heat treatment in vacuum on shungite shielding properties. *Doklady BGUIR*. 2014;8: 31–35. (In Russ., abstract in Eng.). Available at: https://elibrary.ru/item.asp?id=29674388

* *Translated by author of the article*

Информация об авторах

Vladimir Y. Buz'ko, Cand. Sci. (Chem.), Director of the REC "Center for Advanced Technologies and Nanomaterials", Kuban State Technological University (Krasnodar, Russian Federation).
https://orcid.org/0000-0002-6335-0230
buzkonmr@mail.ru

Sergey N. Ivanin, Cand. Sci (Chem), Research Fellow, "Center for Advanced Technologies and Nanomaterials", Kuban State Technological University (Krasnodar, Russian Federation).
https://orcid.org/0000-0001-9352-5970
ivanin18071993@mail.ru

Ivan Y. Shutkin, post-graduate student of the Department of Land Transport and Mechanics, Kuban State Technological University (Krasnodar, Russian Federation).
https://orcid.org/0000-0001-9705-7801
5206606@mail.ru

Alexander I. Goryachko, Research Fellow, "Center for Advanced Technologies and Nanomaterials", Kuban State Technological University (Krasnodar, Russian Federation).
https://orcid.org/0000-0001-6480-353X
alexandr_g_i@mail.ru

Sergey A. Udodov, Cand. Sci. (Tech.), Head of the Department of Production of Building Structures and Structural Mechanics Kuban State Technological University (Krasnodar, Russian Federation).
https://orcid.org/0000-0003-4023-9588
udodov-tec@mail.ru

Alexander V. Ozolin, Research Fellow, "Center for Advanced Technologies and Nanomaterials" Kuban State Technological University (Krasnodar, Russian Federation).
https://orcid.org/0000-0002-0173-1716
ozolinml@yandex.ru

Received 18.07.2022; approved after reviewing 22.09.2022; accepted for publication 15.10.2022; published online 25.03.2023.

Translated by Marina Strepetova
Edited and proofread by Simon Cox